

Regioselectivity in the Scholl Reaction: Mono and Double [7]Helicenes

Mohammad Mosharraf Hossain,* Khushabu Thakur, Marat R. Talipov, Sergey V. Lindeman, Saber Mirzaei,* and Rajendra Rathore

Cite This: *Org. Lett.* 2021, 23, 5170–5174

Read Online

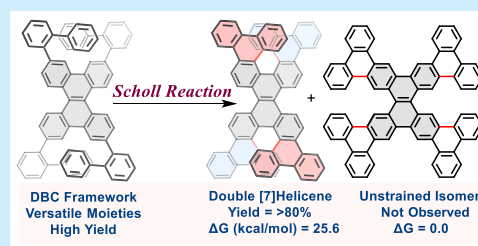
ACCESS |

Metrics & More

Article Recommendations

Supporting Information

ABSTRACT: We employed the density functional theory (DFT)-predicted regioselectivity of the intramolecular Scholl reaction in phenanthrene and dibenzo[*g,p*]chrysene frameworks to obtain π -extended mono and double [7]helicenes, respectively. The formation of these helical structures occurs despite the buildup of a large strain energy up to 30 kcal/mol compared with their most stable isomers. The twisted and strained structures were characterized and analyzed by experimental (NMR, UV–vis, emission, electrochemistry, and single-crystal X-ray diffraction) techniques and were further supported by DFT calculations.

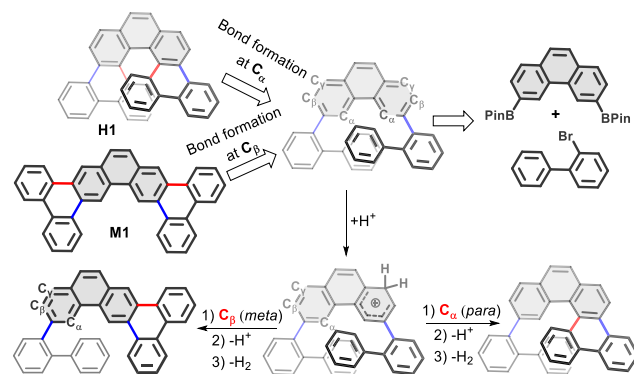


Attempts toward the design and synthesis of polycyclic aromatic hydrocarbons (PAHs) for use as functional materials in electronic and optoelectronic devices continue to increase on account of their potential applications in the ever-developing areas of molecular electronics and photovoltaics.^{1–5} Whereas significant progress has been made in the synthesis of a variety of large planar PAHs, the development of contorted PAHs is challenging, as building up the strain energy, regioselectivity, electronic effects, and so on has to be carefully considered.⁶ Since the first synthesis of [6]helicene (i.e., an ortho-fused, π -conjugated PAH with helical chirality) by Newman and Lednicer in 1956,⁷ extensive efforts have been dedicated toward the progress of efficient and highly inventive synthetic methods for the preparation of helicenes and a number of analogs with helical chirality.^{7–11}

The Scholl reaction, oxidative arene–arene bond formation, is a key reaction for the design and synthesis of PAHs.^{12,13} Durolo and coworkers showed that the intramolecular Scholl reaction can be used, despite the accumulated strain, to form helicenes.¹⁴ Thereafter, the synthesis of several helical compounds showed that this reaction can be used to overcome the built up strain energy.^{15–17} In addition to vast applications, the mechanism of the Scholl reaction, which can occur via arenium ion (proton transfer) or cation radical (electron transfer) mechanisms, has been studied both experimentally and computationally.^{18–20} Despite the existence of these mechanisms, the regioselectivity of the Scholl reaction is not yet fully predictable. In this Letter, the density functional theory (DFT)-predicted regiochemical outcome of bond-forming events is employed in a given substrate based on the arenium ion formation¹⁹ to accomplish a facile synthesis of novel strained and π -extended mono and double [7]helicenes.

A simple retrosynthetic analysis of the [7]helicene derivative H1 (Scheme 1) suggests that it can be synthesized from a

Scheme 1. Retrosynthetic Approach for the [7]Helicene Derivative



phenanthrene framework, available from the substituted phenanthrene boronic ester and 2-bromobiphenyl, by an oxidative C–C bond formation reaction. However, the formation of the helicene requires that oxidative C–C bond formation between biphenyl and phenanthrene moieties occurs at carbons 4 and 5 (denoted as C_α) and not at carbons 2 and 7 (denoted as C_β), which would lead to the planar isomer M1.

According to the arenium cation formation mechanism, the protonation should occur in the ortho or para positions with respect to the newly formed C–C bond;¹⁹ this rule leaves the

Received: May 21, 2021

Published: June 14, 2021



C_γ on the phenanthrene backbone as the only site for the protonation. The next step is the electrophilic attack of the ortho (C_β) or para (C_α) position by the adjacent biphenyl moiety. After the first C–C bond formation, the same pathway is followed by the other side of the molecule (Scheme 1). Indeed, the DFT calculations suggest that C–C bond formation at the carbons C_α has a lower transition-state energy ($\Delta\Delta G \approx 3$ kcal/mol, calculated at the CAM-B3LYP-D3BJ/6-31+G**+PCM(CH₂Cl₂) level of theory; Figures S5 and S6, SI) and should be the major product. This functional and basis set are used throughout this Letter unless otherwise noted. (Computational details are provided in the SI.) However, one may have predicted that the formation of sterically unstrained M1 should be the major product because it is ~ 11.9 kcal/mol more stable than the corresponding helicene H1 (Figure S9, SI). Note that the cation radical mechanism showed similar regioselectivity but higher barriers (~ 8 kcal/mol; Figures S7 and S8, SI), and thus we believe that the arenium ion mechanism is a more feasible reaction pathway.

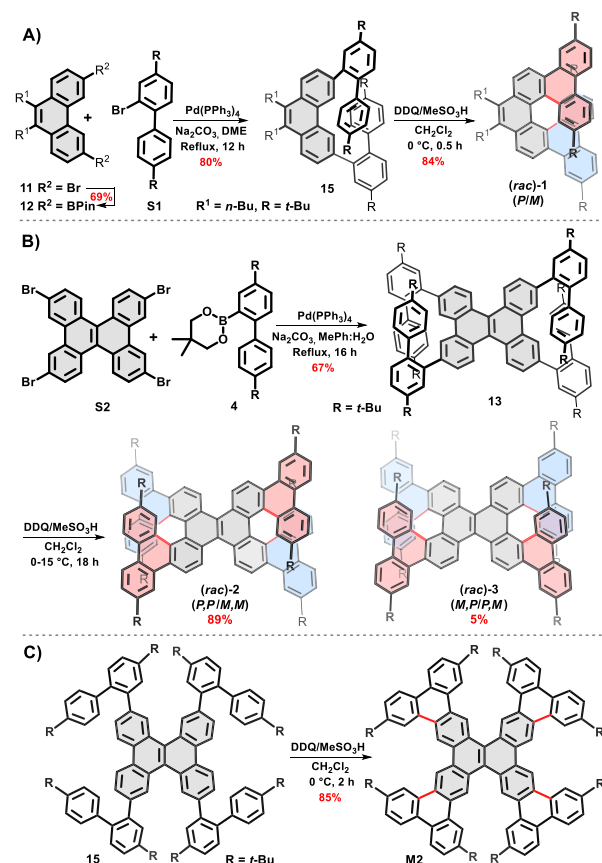
To assess our hypothesis that cyclization at C_α is preferred despite the buildup of strain energy, we followed a systematic synthetic approach. The strategy for the preparation of helicene 1 starts with the seven-step synthesis of 3,6-dibromo-9,10-dibutyl-phenanthrene 11 from the readily available 2-bromobenzoyl chloride in $\sim 55\%$ overall yield. (See the Supporting Information for full details.) To make 11 a suitable coupling partner for the Suzuki–Miyaura cross-coupling reaction, the bromines were converted to boronate ester (BPin) 12 in 69% yield and reacted with 2-bromo-4,4'-di-*tert*-butylbiphenyl S1²¹ using Pd(PPh₃)₄ as the catalyst to afford compound 15 in 80% yield (Scheme 2A). Note that *t*-butyl groups are added to increase the solubility of the product.

Finally, the oxidative C–C bond formation reaction was completed using 2,3-dichloro-5,6-dicyano-1,4-benzoquinone (DDQ) and MeSO₃H in CH₂Cl₂ at 0 °C for <1 h.²² In agreement with our hypothesis, only the helicene 1 was observed as the product in excellent isolated yield ($\sim 84\%$), and no planar isomer (M1) was observed. The structure of π -extended [7]helicene 1 was confirmed by NMR and single-crystal X-ray crystallography. (See the crystallography section and the Supporting Information.)

Encouraged by these results, we considered the possibility of the synthesis of a double [7]helicene. The simple retrosynthetic analysis of [7]helicene (Scheme 1) suggests that double analogs can be synthesized from a dibenzo[*g,p*]-chrysene (DBC) derivative, which is essentially a combination of mirror images of phenanthrene. The desired double [7]helicene is much higher in energy ($\Delta G = 25.6$ kcal/mol; Figure S10, SI) than the thermodynamically more stable isomer M2 (Scheme 2C). To address this challenge, we undertook the synthesis.

DBC has been brominated in quantitative yield to afford the 3,6,11,14-tetrabromodibenzo[*g,p*]chrysene S2.²³ The Suzuki–Miyaura cross-coupling reaction of S2 with four equivalents of biphenyl boronic ester 4 has generated the important precursor 13 in 67% yield, which allowed us to carry out the final step, oxidative C–C bond formation using DDQ/MeSO₃H in CH₂Cl₂ at 0 °C, as shown in Scheme 2B. As expected by looking at the structure of the double [7]helicene derivatives, two different relative configurations (P,P/M,M and M,P/P,M) are synthetically feasible. Fortunately, we were able to isolate and identify them. The major and minor products were

Scheme 2. Synthetic Approaches for (A) Mono [7]helicene 1, (B) Double [7]helicenes 2 and 3, and (C) Controlled Molecule M2



identified as the P,P/M,M (2) and M,P/P,M (3) configurations, respectively; note that 3 is ~ 4.7 kcal/mol less stable than 2 (Figure S10, SI). To prove that no nonhelical isomer was present in our mixture, the synthesis of compound M2 has been accomplished starting from the 2,7,10,15-tetrabromodibenzo[*g,p*]chrysene S3.²³ As provided in the SI (Figure S4), the NMR spectrum of this compound is distinct, and no trace of this chemical shift pattern was observed in the double-helicene reaction.

The crystal structures of mono (1) and double [7]helicenes (2 and 3) are depicted in the Figure 1. In the mono [7]helicene 1, the center-to-center distance between the overlapped terminal phenyl rings is ~ 3.8 Å which is more than twice the van der Waals radius of a carbon atom (~ 1.7 Å). Comparing these values with the crystal structure of normal [7]helicene (i.e., neither extended nor substituted, 3.8 Å)²⁴ shows that the extension of the π system or substitution did not affect the general geometry of 1. The distance between the CH₃ carbon of the *t*-butyl group and the center of the extended phenyl ring is as short as ~ 3.5 Å for 1. Also, the attached biphenyl moieties undergo contortion after oxidative C–C bond formation. Analyzing the crystal structure of 2 shows that the center-to-center distance of the terminal rings increases to ~ 4.2 Å (average of two helicenes); this value is ~ 4.1 Å for 3. The bigger values, compared with 1, can be attributed to the twisted nature of the DBC framework, which is not planar like the phenanthrene in 1. This effect also reveals itself in the *t*-Bu CH₃ carbon-to-phenyl ring distance, which increases to ~ 3.7 Å for both 2 and 3.

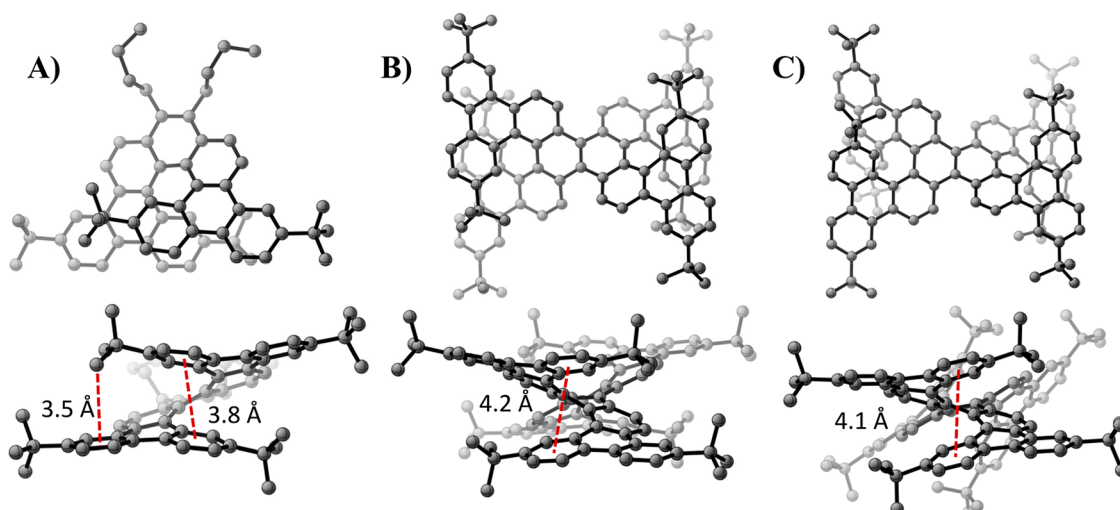


Figure 1. Top view (up) and front view (down) of crystal structures (obtained at 100 K) of (A) mono[7]helicene **1**, (B) double [7]helicene **2** (P,P/M,M), and (C) double [7]helicene **3** (P,M/M,P). Hydrogens and solvent molecules are deleted for clarity.

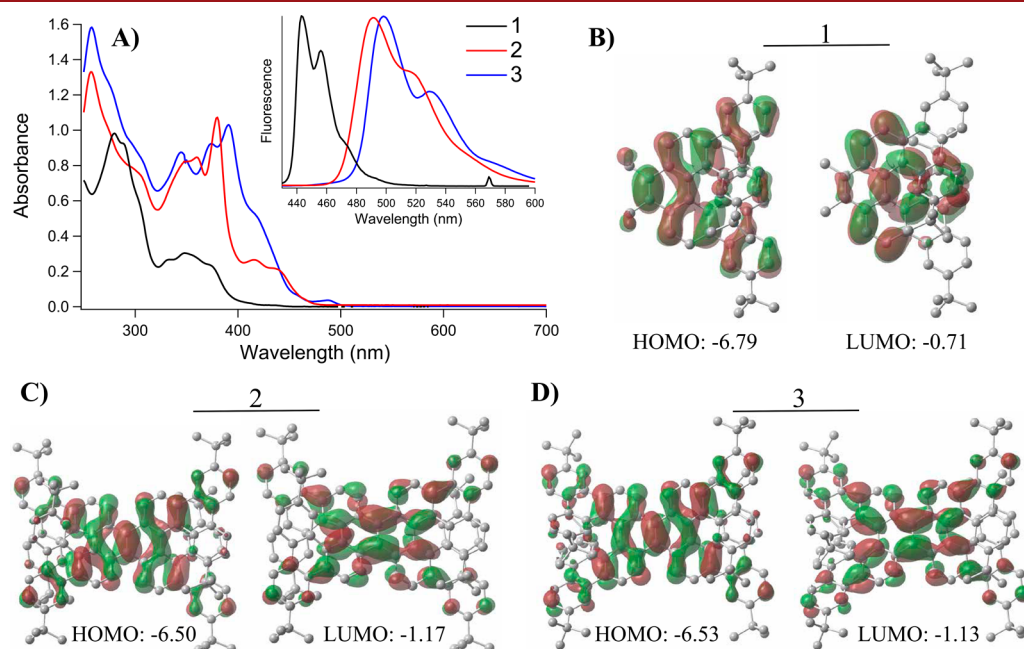


Figure 2. (A) Compilation of absorption and normalized emission spectra of **1**, **2**, and **3** in CH_2Cl_2 at 22 °C. HOMO and LUMO (± 0.02 au) of (B) **1**, (C) **2**, and (D) **3** and their DFT-calculated energies in electronvolts.

To elucidate the effects of molecular geometry on the frontier molecular orbitals of these helicenes, we measured the UV–visible absorption, fluorescence emission, and electrochemical properties and further supported them by DFT calculations. **Figure 2** shows the compiled UV–vis absorption and fluorescence emission spectra of **1**, **2**, and **3** in CH_2Cl_2 at 22 °C.

Comparing the sharp and distinct UV–vis peaks of compounds **2** and **3** indicates a clear red shift from 380 to 391 nm (**Figure 2A**). This red shift is also obvious by comparing their emission spectra; the λ_{em} is 477 nm for **2** and 498 nm for molecule **3**. Also, the mono [7]helicene **1** shows the lowest values ($\lambda_{\text{max}} = 348$ and $\lambda_{\text{em}} = 444$ nm) among all three studied molecules, which can be attributed to the less-extended π -system that increases its HOMO–LUMO gap (E_g , **Table 1**).

Table 1. Comparison among **1**, **2**, and **3**

	compound		
	1	2	3
$E_{1/2}$ (V vs Fc/Fc ⁺)	0.74	0.60	0.58
E_{HOMO} (eV) ^a	−5.54	−5.40	−5.38
E_{HOMO} (eV) ^b	−6.79	−6.50	−6.53
E_{LUMO} (eV) ^b	−0.71	−1.17	−1.13
E_g (eV) ^b	6.08	5.33	5.40
strain energy (kcal/mol) ^b	11.9	25.6	30.3

^aCalculated using experimental data²⁸ ($E_{\text{HOMO}} = -[E_{1/2} + 4.80]$ eV).

^bFrontier molecular orbitals and strain energies calculated at the CAM-B3LYP-D3BJ/6-31+G**+PCM(CH_2Cl_2) level of theory.

(TD-)DFT calculations were employed to have better insights into the optical features of these molecules. The

calculated energies of the frontier molecular orbitals of all three helicenes showed a decreasing trend of E_g ($E_g = E_{\text{LUMO}} - E_{\text{HOMO}}$) by moving from mono to double helicenes. This difference is as big as 0.71 eV. (See Figure 2 and Table 1.) In addition, the TD-DFT calculations correctly simulated the observed red shift of the UV-vis spectrum of **3** compared with **2** (Figures S12 and S13). The strongest transition is ~ 331.5 (oscillator strength = 2.6) and 341.3 nm (oscillator strength = 2.1) for **2** and **3**, respectively. The highest calculated transition is 388.4 and 390.9 nm for **2** and **3**, respectively, with weaker oscillator strengths. This band (390.9 nm) is coming from a combination of HOMO to LUMO+1 (59%) and HOMO-1 to LUMO (25%) transitions for molecule **3**, whereas the HOMO-to-LUMO (89%) transition is the major contributor to the calculated 388.4 nm band of **2**.

Electrochemical studies showed reversible (for **1**) and quasireversible (for **2** and **3**) oxidation events in dichloromethane with tetrabutylammonium hexafluorophosphate (TBAPF₆) as a supporting electrolyte. The oxidation potentials (E_{ox}) of **1**, **2**, and **3** were observed at 0.74, 0.60, and 0.58 V vs Fc/Fc⁺, respectively (Figure 3). Similar to the red shift of the

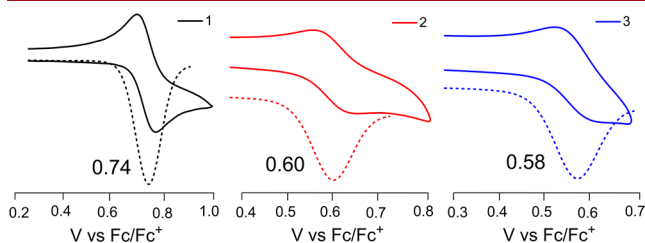


Figure 3. Cyclic (—) and square-wave (⋯) voltammograms of **1**, **2**, and **3** in CH₂Cl₂ at a scan rate of 100 mV s⁻¹ and 22 °C.

UV-vis and emission spectra, the decrease in the E_{ox} value (~ 150 mV) when moving from the mono to more π -extended double [7]helicene was expected. This effect has been observed in almost all conjugated molecules and has been attributed to the better hole (positive charge) delocalization in more extended systems.^{25,26} However, this decrease will finally converge due to the interplay between the electronic coupling and the reorganization energy of the molecule.²⁷ The almost identical E_{ox} values for **2** and **3** can be justified based on the shape and energy of the HOMO of **2** and **3**. The HOMO is mainly distributed over the DBC backbone, and unlike **1**, it has a small contribution over the biphenyl moieties for both double [7]helicenes. Moreover, the DFT-calculated HOMO energies reveal very close values that are in good agreement with the experimental values (Table 1) obtained by employing $E_{1/2}$ of the first oxidation event according to $E_{\text{HOMO}} = -[E_{1/2} + 4.80]$ eV.²⁸ Comparing the redox properties of **2** and **3** with DBC (the first oxidation potential of DBC is ~ 0.88 V vs Fc/Fc⁺)²⁹ shows that fusing four biphenyl moieties into the DBC backbone can decrease the first oxidation potential around 0.29 V.

In summary, the DFT data, according to the arenium cation formation mechanism, revealed that the para position of the protonated carbon is more reactive and is the site of the new intramolecular C-C bond formation in the phenanthrene and dibenzo[*g,p*]schrysenes frameworks. According to this prediction, we have developed the synthesis of novel and π -extended mono and double [7]helicenes by employing the regioselectivity of intramolecular C-C bond formation in the Scholl

reaction. The formation of these molecules was observed despite the generation of strain energy up to 30 kcal/mol compared with their unstrained isomers. The structures of all synthesized helicenes were characterized and carefully analyzed using NMR, UV-vis, and emission spectroscopy, single-crystal X-ray diffraction, and DFT calculations. Therefore, we believe that the established synthetic protocol here can help chemists to design and access unrevealed twisted and π -extended aromatic systems with unusual electronic properties and help them to predict the regioselectivity of the Scholl reaction.

■ ASSOCIATED CONTENT

Supporting Information

The Supporting Information is available free of charge at <https://pubs.acs.org/doi/10.1021/acs.orglett.1c01706>.

Procedures for the synthesis, NMR spectra, and computational details(PDF)

Accession Codes

CCDC 2084553–2084555 contain the supplementary crystallographic data for this paper. These data can be obtained free of charge via www.ccdc.cam.ac.uk/data_request/cif, or by emailing data_request@ccdc.cam.ac.uk, or by contacting The Cambridge Crystallographic Data Centre, 12 Union Road, Cambridge CB2 1EZ, UK; fax: +44 1223 336033.

■ AUTHOR INFORMATION

Corresponding Authors

Mohammad Mosharraf Hossain – Department of Chemistry, Marquette University, Milwaukee, Wisconsin 53201-1414, United States; Present Address: M.M.H.: Miami University, Department of Chemistry and Biochemistry, Oxford, Ohio 45056, United States.; orcid.org/0000-0002-6996-4209; Email: hossaimm@miamioh.edu

Saber Mirzaei – Department of Chemistry, University of Pittsburgh, Pittsburgh, Pennsylvania 15260, United States.; orcid.org/0000-0001-9651-9197; Email: saber.mirzaei@pitt.edu

Authors

Khushabu Thakur – Department of Chemistry, Marquette University, Milwaukee, Wisconsin 53201-1414, United States

Marat R. Talipov – Department of Chemistry, Marquette University, Milwaukee, Wisconsin 53201-1414, United States; Present Address: M.R.T.: Department of Chemistry and Biochemistry, New Mexico State University, Las Cruces, NM 88003, United States.; orcid.org/0000-0002-7559-9666

Sergey V. Lindeman – Department of Chemistry, Marquette University, Milwaukee, Wisconsin 53201-1414, United States

Rajendra Rathore – Department of Chemistry, Marquette University, Milwaukee, Wisconsin 53201-1414, United States.; orcid.org/0000-0001-7387-7936

Complete contact information is available at: <https://pubs.acs.org/doi/10.1021/acs.orglett.1c01706>

Notes

The authors declare no competing financial interest.
[†]R.R.: Deceased February 16, 2018.

ACKNOWLEDGMENTS

We thank Prof. C. Scott Hartley (Miami University), Prof. Scott A. Reid (Marquette University), and Prof. Raúl Hernández Sánchez (University of Pittsburgh) for helpful discussions and encouragement. We also thank the NSF (CHE-1508677) for financial support. S.M. acknowledges the support from the Dietrich School of Arts & Sciences Graduate Fellowship.

REFERENCES

- (1) Yano, Y.; Mitoma, N.; Ito, H.; Itami, K. A Quest for Structurally Uniform Graphene Nanoribbons: Synthesis, Properties, and Applications. *J. Org. Chem.* **2020**, *85* (1), 4–33.
- (2) Watson, M. D.; Fechtenkötter, A.; Müllen, K. Big Is Beautiful—“Aromaticity” Revisited from the Viewpoint of Macromolecular and Supramolecular Benzene Chemistry. *Chem. Rev.* **2001**, *101* (5), 1267–1300.
- (3) Li, C.; Liu, M.; Pschirer, N. G.; Baumgarten, M.; Müllen, K. Polyphenylene-Based Materials for Organic Photovoltaics. *Chem. Rev.* **2010**, *110* (11), 6817–6855.
- (4) Roncali, J.; Leriche, P.; Blanchard, P. Molecular Materials for Organic Photovoltaics: Small is Beautiful. *Adv. Mater.* **2014**, *26* (23), 3821–3838.
- (5) Heath, J. R. Molecular Electronics. *Annu. Rev. Mater. Res.* **2009**, *39* (1), 1–23.
- (6) Ball, M.; Zhong, Y.; Wu, Y.; Schenck, C.; Ng, F.; Steigerwald, M.; Xiao, S.; Nuckolls, C. Contorted Polycyclic Aromatics. *Acc. Chem. Res.* **2015**, *48* (2), 267–276.
- (7) Newman, M. S.; Lednicer, D. The Synthesis and Resolution of Hexahelicene. *J. Am. Chem. Soc.* **1956**, *78* (18), 4765–4770.
- (8) Shen, Y.; Chen, C.-F. Helicenes: Synthesis and Applications. *Chem. Rev.* **2012**, *112* (3), 1463–1535.
- (9) Stará, I. G.; Starý, I. Helically Chiral Aromatics: The Synthesis of Helicenes by [2 + 2 + 2] Cycloisomerization of π -Electron Systems. *Acc. Chem. Res.* **2020**, *53* (1), 144–158.
- (10) Gingras, M. One hundred years of helicene chemistry. Part 1: non-stereoselective syntheses of carbohelicenes. *Chem. Soc. Rev.* **2013**, *42* (3), 968–1006.
- (11) Li, C.; Yang, Y.; Miao, Q. Recent Progress in Chemistry of Multiple Helicenes. *Chem. - Asian J.* **2018**, *13* (8), 884–894.
- (12) Grzybowski, M.; Skonieczny, K.; Butenschön, H.; Gryko, D. T. Comparison of Oxidative Aromatic Coupling and the Scholl Reaction. *Angew. Chem., Int. Ed.* **2013**, *52* (38), 9900–9930.
- (13) Grzybowski, M.; Sadowski, B.; Butenschön, H.; Gryko, D. T. Synthetic Applications of Oxidative Aromatic Coupling—From Biphenols to Nanographenes. *Angew. Chem., Int. Ed.* **2020**, *59* (8), 2998–3027.
- (14) Pradhan, A.; Dechambenoit, P.; Bock, H.; Durolo, F. Highly Twisted Arenes by Scholl Cyclizations with Unexpected Regioselectivity. *Angew. Chem., Int. Ed.* **2011**, *50* (52), 12582–12585.
- (15) Hu, Y.; Wang, X.-Y.; Peng, P.-X.; Wang, X.-C.; Cao, X.-Y.; Feng, X.; Müllen, K.; Narita, A. Benzo-Fused Double [7]-Carbohelicene: Synthesis, Structures, and Physicochemical Properties. *Angew. Chem., Int. Ed.* **2017**, *56* (12), 3374–3378.
- (16) Fujikawa, T.; Segawa, Y.; Itami, K. Synthesis and Structural Features of Quadruple Helicenes: Highly Distorted π Systems Enabled by Accumulation of Helical Repulsions. *J. Am. Chem. Soc.* **2016**, *138* (10), 3587–3595.
- (17) Reger, D.; Haines, P.; Heinemann, F. W.; Guldi, D. M.; Jux, N. Oxa[7]superhelicene: A π -Extended Helical Chromophore Based on Hexa-peri-hexabenzocoronenes. *Angew. Chem., Int. Ed.* **2018**, *57* (20), 5938–5942.
- (18) Clowes, G. A. Studies of the Scholl reaction: oxidative dehydrogenation involving 1-ethoxynaphthalene and related compounds. *J. Chem. Soc. C* **1968**, No. 0, 2519–2526.
- (19) Rempala, P.; Kroulik, J.; King, B. T. Investigation of the Mechanism of the Intramolecular Scholl Reaction of Contiguous Phenylbenzenes. *J. Org. Chem.* **2006**, *71* (14), 5067–5081.
- (20) Zhai, L.; Shukla, R.; Wadumethrige, S. H.; Rathore, R. Probing the Arenium-Ion (ProtonTransfer) versus the Cation-Radical (Electron Transfer) Mechanism of Scholl Reaction Using DDQ as Oxidant. *J. Org. Chem.* **2010**, *75* (14), 4748–4760.
- (21) Kim, Y.-H.; Kim, H.-S.; Kwon, S.-K. Synthesis and Characterization of Highly Soluble and Oxygen Permeable New Polyimides Based on Twisted Biphenyl Dianhydride and Spirofluorene Diamine. *Macromolecules* **2005**, *38* (19), 7950–7956.
- (22) Scholl, R.; Mansfeld, J. meso-Benzodanthron (Helianthron), meso-Naphthodanthron, und ein neuer Weg zum Flavanthron. *Ber. Dtsch. Chem. Ges.* **1910**, *43* (2), 1734–1746.
- (23) Hossain, M. M.; Mirzaei, M. S.; Lindeman, S.; Mirzaei, S.; Rathore, R. π -Extended dibenzo[gp]chrysenes. *Org. Chem. Front.* **2021**, *8*, 2393–2401.
- (24) Fuchter, M. J.; Weimar, M.; Yang, X.; Judge, D. K.; White, A. J. P. An unusual oxidative rearrangement of [7]-helicene. *Tetrahedron Lett.* **2012**, *53* (9), 1108–1111.
- (25) Hossain, M. M.; Ivanov, M. V.; Wang, D.; Reid, S. A.; Rathore, R. Spreading Electron Density Thin: Increasing the Chromophore Size in Polyaromatic Wires Decreases Interchromophoric Electronic Coupling. *J. Phys. Chem. C* **2018**, *122* (31), 17668–17675.
- (26) Boddada, A.; Hossain, M. M.; Saeed Mirzaei, M.; Lindeman, S. V.; Mirzaei, S.; Rathore, R. Angular ladder-type meta-phenylenes: synthesis and electronic structural analysis. *Org. Chem. Front.* **2020**, *7* (20), 3215–3222.
- (27) Ivanov, M. V.; Talipov, M. R.; Boddada, A.; Abdelwahed, S. H.; Rathore, R. Hückel Theory + Reorganization Energy = Marcus–Hush Theory: Breakdown of the 1/n Trend in π -Conjugated Poly-p-phenylene Cation Radicals Is Explained. *J. Phys. Chem. C* **2017**, *121* (3), 1552–1561.
- (28) Cardona, C. M.; Li, W.; Kaifer, A. E.; Stockdale, D.; Bazan, G. C. Electrochemical Considerations for Determining Absolute Frontier Orbital Energy Levels of Conjugated Polymers for Solar Cell Applications. *Adv. Mater.* **2011**, *23* (20), 2367–2371.
- (29) Ivanov, M. V.; Talipov, M. R.; Navale, T. S.; Rathore, R. Ask Not How Many, But Where They Are: Substituents Control Energetic Ordering of Frontier Orbitals/Electronic Structures in Isomeric Methoxy-Substituted Dibenzochrysenes. *J. Phys. Chem. C* **2018**, *122* (5), 2539–2545.